

The dynamics of scalar-tensor cosmology from RS two-brane model

Laur Järv,¹ Piret Kuusk,² Margus Saal³

Institute of Physics, University of Tartu, Riia 142, Tartu 51014, Estonia

Abstract

We consider a Randall-Sundrum two-brane cosmological model in the low energy gradient expansion approximation by Kanno and Soda. It is a scalar-tensor theory with a specific coupling function and a specific potential. Upon introducing the FLRW metric and perfect fluid matter on both branes in the Jordan frame, the effective dynamical equation for the the A-brane (our Universe) scale factor decouples from the scalar field and B-brane matter leaving only a non-vanishing integration constant (the dark radiation term). We find exact solutions for the A-brane scale factor for four types of matter: cosmological constant, radiation, dust, and cosmological constant plus radiation. We perform a complementary analysis of the dynamics of the scalar field (radion) using phase space methods and examine convergence towards the limit of general relativity. In particular, we find that radion stabilizes at a certain finite value for suitable negative matter densities on the B-brane. Observational constraints from Solar system experiments (PPN) and primordial nucleosynthesis (BBN) are also briefly discussed.

Key words: two-brane cosmology, scalar-tensor theory in the Jordan frame, phase space methods, observational constraints

¹ Electronic address: laur@fi.tartu.ee

² Electronic address: piret@fi.tartu.ee

³ Electronic address: margus@hexagon.fi.tartu.ee

1 Introduction

A great challenge for contemporary theoretical cosmology is to find and examine possible frameworks for explaining new observational data (dark energy, accelerated expansion, etc.) which may not be accommodated in the standard cosmological model based on the Friedmann solution of the Einstein equations. Investigations of alternative cosmological models include the braneworld scenario, where our visible Universe is one of the two hypersurfaces embedded in a 5-dimensional bulk spacetime, while the proper distance between the branes is measured by the radion field.

The first phenomenological braneworld models were presented by Randall and Sundrum [1, 2] in order to solve the hierarchy problem of the Standard Model of particle physics. A more fundamental theoretical setup for braneworlds arises in the 10-dimensional superstring theory (or the 11-dimensional M-theory) with 5 (6) compactified dimensions leaving us a 5-dimensional cosmological bulk spacetime [3]. In models with several branes which move in the bulk, a collision of the branes can mimic the big bang [4] or the exit from inflation [5]. There are at least two approaches to get a 4-dimensional effective theory from the 5-dimensional theory. The first one, developed by Kanno and Soda [6, 7], is the gradient expansion method where the brane tension is taken to be much bigger than the energy density on the brane. The second approach, developed by Brax et al. [8], is known as the moduli space approximation. In this approach the brane positions are described by scalar moduli fields emerging from compactification assuming that the motion of the branes is slow. It can be shown that at least at the first order both approximations agree [9].

Following Kanno and Soda [7], we consider the Randall-Sundrum type I cosmological scenario [1] with two branes (A and B) moving in a 5-dimensional bulk. Both branes are taken to be homogeneous and isotropic, and supporting energy-momentum tensors of a perfect barotropic fluid, with barotropic index Γ on the A-brane (identified with our visible Universe) and Γ^B on the B-brane. The field equations of the effective 4-dimensional theory obtained by Kanno and Soda [7] are the equations of a scalar-tensor theory with one scalar field (interpreted as a radion) with a specific coupling function $\omega(\Psi)$.

In recent decades, a lot of work has been done on studying scalar-tensor cosmologies with non-constant coupling function $\omega(\Psi)$. The general properties of the evolution of Ψ in the Einstein frame were investigated by Damour and Nordtvedt [10] and in the Jordan frame by Serna et al. [11], while an analogous study in the case of a massive scalar field was presented by Santiago et al. [12]. A comprehensive analysis of the early and late time cosmological models in the Jordan frame was carried out by Barrow and Parsons [13]. Various observational constraints on scalar-tensor cosmologies were discussed by Santiago et al. [14], Damour and Pichon [15], Clifton et al. [16], and Coc et al. [17], and for models with two branes by Palma [18]. In these papers, most calculations are performed in the unphysical Einstein frame, although the Jordan frame is used for physical interpretations.¹

¹For a lucid explanation of the relevance and relationship of the two frames, as well as a general review

The scalar-tensor cosmological model we consider in the Jordan frame stands out from those mentioned above in three respects. First, the second brane can contain matter and its matter tensor acts as an additional source in the equations of the gravitational and the scalar field. Second, the coupling function of the scalar field has a specific form $\omega(\Psi) = \frac{3\Psi}{2(1-\Psi)}$ which is fixed by the construction of the model. Third, there are possible cosmological constants on both branes appearing via a specific potential of the scalar field, so in general we consider two-component source terms (matter + cosmological constants on both branes).

The cosmology of this model was first investigated by Kanno et al. [20] and later also by us [21].² In this paper we obtain several new general analytic solutions for the flat ($k = 0$) A-brane scale factor, thus encompassing solutions for all interesting matter tensors: 1) cosmological constants and no matter, 2) radiative matter and no cosmological constants, 3) dust matter and no cosmological constants, as well as 4) radiative matter and cosmological constants. We also find the accompanying analytic solutions for the radion field in cases 2) and 4) above. We apply the methods of dynamical systems to study the evolution of the radion field, finding fixed points and drawing phase portraits related to the first three cases. The global picture emerging from this analysis is more clear and has some advantages over the usual procedure of studying the convergence of scalar-tensor theories towards general relativity, which relies on an analogy with a fictitious particle with velocity dependent effective mass [10, 11, 12]. Depending on the type and the (initial) density of A- and B-brane matter, the branes typically evolve towards infinite separation or to a collision, but for certain negative B-brane energy densities, the radion (corresponding to the inter-brane distance) is stabilized by an attractor at a certain finite value. Finally, we consider Solar system experiments and Big Bang nucleosynthesis to derive some observational limits on the parameters of the model.

The plan of the paper is as follows. Sects. 2 and 3 give the basic equations of the model and clarify their general properties. Sect. 4 presents the analytic solutions, while Sect. 5 carries out a complementary analysis of the dynamics of the scalar field. Sect. 6 follows with a brief discussion on observational constraints, and Sect. 7 contains some concluding remarks.

2 Effective action and field equations in the Jordan frame

The starting point is the 5-dimensional Randall-Sundrum action [1]

$$I_{RS} = \frac{1}{2\kappa_5^2} \int d^5x \sqrt{-g} (\mathcal{R} - 2\Lambda_5) + \int d^4x \sqrt{-h} (\mathcal{L}_m - \Sigma) + \int d^4x \sqrt{-f} (\mathcal{L}_m^B - \Sigma^B), \quad (1)$$

of scalar-tensor cosmology, see the recent book by Faraoni [19].

²The cosmology and radion dynamics of RS two-brane model has been studied by many authors using various approaches [22], the closest to ours being the moduli space approximation [8, 23, 24].

where \mathcal{R} is the scalar curvature, while $h_{\mu\nu}$ and $f_{\mu\nu}$ are the induced metrics on the A- and B-brane, respectively. We assume that the brane tensions can be divided into two parts

$$\Sigma = \sigma_0 + \sigma, \quad \Sigma^B = \sigma_0^B + \sigma^B, \quad (2)$$

with $|\sigma_0| \gg |\sigma|$, $|\sigma_0^B| \gg |\sigma^B|$. The first part is balanced with the bulk cosmological constant Λ_5 ,

$$(\sigma_0)^2 = (\sigma_0^B)^2 = -\frac{6\Lambda_5}{\kappa_5^2}, \quad \Lambda_5 \equiv -\frac{6}{\ell^2}, \quad (3)$$

where ℓ is the curvature radius of 5-dimensional bulk anti-de Sitter spacetime. The second part gives rise to unbalanced energy density on the branes which can be interpreted in terms of effective cosmological constants λ , λ^B as

$$\sigma = \frac{\lambda c^2}{\kappa^2}, \quad \sigma^B = \frac{\lambda^B c^2}{\kappa^2}. \quad (4)$$

Let us introduce a dimensionless scalar field Ψ , called radion, which measures the proper orthogonal distance between the branes situated at $y = 0$ and $y = \ell$ (at the fixed points of S_1/Z_2 orbifold spacetime),

$$d(x) \equiv \int_0^\ell \sqrt{g_{55}} dy = -\frac{\ell}{2} \ln(1 - \Psi), \quad \Psi \in [0, 1], \quad (5)$$

in coordinates where $g_{55} = g_{55}(x)$. Then, according to the low energy expansion scheme developed by Kanno and Soda, in a sense that the energy density of the matter on the brane is smaller than the brane tension $|\rho/\Sigma| \ll 1$, $|\rho^B/\Sigma^B| \ll 1$, the 4-dimensional field equations on the A-brane can be written as [7]

$$G^\mu{}_\nu(h) = \frac{\kappa^2}{\Psi} [T^{A\mu}{}_\nu(h) + (1 - \Psi)^2 T^{B\mu}{}_\nu(f)] - \frac{\kappa^2}{\Psi} \delta^\mu{}_\nu [\sigma + (1 - \Psi)^2 \sigma^B] + \frac{1}{\Psi} (\Psi|^\mu{}_{|\nu} - \delta^\mu{}_\nu \Psi|^\alpha{}_{|\alpha}) + \frac{\omega(\Psi)}{\Psi^2} (\Psi|^\mu \Psi|_\nu - \frac{1}{2} \delta^\mu{}_\nu \Psi|^\alpha \Psi|_\alpha), \quad (6)$$

$$\Psi|^\mu{}_{|\mu} = \frac{\kappa^2}{2\omega + 3} [T^A(h) + (1 - \Psi) T^B(f)] - \frac{4\kappa^2}{2\omega + 3} [\sigma + (1 - \Psi) \sigma^B] - \frac{1}{2\omega + 3} \frac{d\omega}{d\Psi} \Psi|^\mu \Psi|_\mu, \quad (7)$$

where $|$ denotes the covariant derivative with respect to the A-brane metric $h_{\mu\nu}$ and $\kappa^2 \equiv \kappa_5^2/\ell$ is the 4-dimensional bare gravitational constant. The brane metrics are conformally related by $f_{\mu\nu} = (1 - \Psi)h_{\mu\nu}$ while the function

$$\omega(\Psi) \equiv \frac{3}{2} \frac{\Psi}{1 - \Psi} \quad (8)$$

describes the proper distance d between the branes as (cf. [25])

$$\omega = \frac{3}{2} (e^{2\frac{d}{\ell}} - 1). \quad (9)$$

It is noteworthy that Eqs. (6) and (7) coincide with the equations of the general scalar-tensor theory with a specific form (8) of the coupling function $\omega(\Psi)$ and an extra

matter term from the B-brane. These equations can be derived from the 4-dimensional scalar-tensor action

$$I_{JF}^A = \frac{1}{2\kappa^2} \int d^4x \sqrt{-h} \left[\Psi R(h) - \frac{\omega(\Psi)}{\Psi} \Psi^{|\alpha} \Psi_{|\alpha} - 2\kappa^2 V(\Psi) \right] \\ + \int d^4x \sqrt{-h} \mathcal{L}_m^A + \int d^4x \sqrt{-h} (1 - \Psi)^2 \mathcal{L}_m^B, \quad (10)$$

where $\omega(\Psi)$ is given by (8) and $V(\Psi)$ denotes an effective potential introduced by cosmological constants on the branes,

$$V(\Psi) = \sigma + \sigma^B (1 - \Psi)^2. \quad (11)$$

If $\mathcal{L}_m^B \equiv 0$ and $\sigma^B = 0$, the influence of the B-brane disappears from the action and we are left with scalar-tensor a theory with a constant potential $V = \sigma$. The Eqs. (6) and (7) reduce to Einstein's general relativity when $\dot{\Psi} = 0$, $\Psi = 1$, i.e., at $\omega(\Psi) \rightarrow \infty$, $d \rightarrow \infty$.

3 FLRW type two-brane cosmology

3.1 Field equations

Assuming that in the Jordan frame the Universe on the A-brane is described by the FLRW line element

$$ds^2 = -dt^2 + a^2(t) \left[\frac{dr^2}{1 - kr^2} + r^2 (d\theta^2 + \sin^2 \theta d\varphi^2) \right], \quad k = 0, \pm 1, \quad (12)$$

and the matter on the branes is modeled by a perfect barotropic fluid with respect to the corresponding brane metric

$$T_{\mu\nu}^A = (\rho + p) u_\mu u_\nu + p h_{\mu\nu}, \quad p = (\Gamma - 1)\rho, \quad (13)$$

$$T_{\mu\nu}^B = (\rho^B + p^B) u_\mu^B u_\nu^B + p^B f_{\mu\nu}, \quad p^B = (\Gamma^B - 1)\rho^B, \quad (14)$$

we can write the 4-dimensional field equations (6) and (7) as follows:

$$H^2 = -H \frac{\dot{\Psi}}{\Psi} + \frac{1}{4} \frac{\dot{\Psi}^2}{\Psi(1 - \Psi)} + \frac{\kappa^2 V}{3 \Psi} + \frac{\kappa^2 \rho}{3 \Psi} + \frac{\kappa^2 (1 - \Psi)^2}{3 \Psi} \rho^B - \frac{k}{a^2}, \quad (15)$$

$$2\dot{H} + 3H^2 = -\frac{\kappa^2}{\Psi} p - \frac{\kappa^2}{\Psi} (1 - \Psi)^2 p^B + \frac{\kappa^2}{\Psi} V - \frac{\ddot{\Psi}}{\Psi} - 2H \frac{\dot{\Psi}}{\Psi} - \frac{3}{4} \frac{\dot{\Psi}^2}{\Psi(1 - \Psi)} - \frac{k}{a^2}, \quad (16)$$

$$\ddot{\Psi} = -3H\dot{\Psi} - \frac{1}{2} \frac{\dot{\Psi}^2}{(1 - \Psi)} + \frac{2}{3} \kappa^2 \left(2V - \Psi \frac{dV}{d\Psi} \right) (1 - \Psi) \\ + \frac{\kappa^2}{3} (1 - \Psi) (\rho - 3p) + \frac{\kappa^2}{3} (1 - \Psi)^2 (\rho^B - 3p^B). \quad (17)$$

In the case $\dot{\Psi} = 0$, $\Psi = 1$ these reduce to the general relativistic FLRW equations with cosmological constant and barotropic perfect fluid. Note that since cosmological constant is included separately, its modeling by barotropic index $\Gamma = 0$ is redundant.

The Bianchi identity yields the following equations (conservation laws) for the matter fluids:

$$\dot{\rho} + 3H\Gamma\rho = 0 \quad \Rightarrow \quad \rho = \rho_0 \left(\frac{a}{a_0}\right)^{-3\Gamma}, \quad (18)$$

$$\dot{\rho}^B + 3H\Gamma^B\rho^B - \frac{3}{2}\frac{\dot{\Psi}}{(1-\Psi)}\Gamma^B\rho^B = 0 \quad \Rightarrow \quad \rho^B = \rho_0^B \left(\sqrt{\frac{1-\Psi}{1-\Psi_0}}\frac{a}{a_0}\right)^{-3\Gamma^B} \quad (19)$$

(here we assume that $\rho/\rho_0 > 0$, $\rho^B/\rho_0^B > 0$, allowing the possibility of exotic negative energy density on the B-brane). Combining Eq. (18) with Eq. (19) we get a relation between the energy densities on both branes

$$\rho^B = \rho_0^B \left(\frac{1-\Psi}{1-\Psi_0}\right)^{-\frac{3}{2}\Gamma^B} \left(\frac{\rho}{\rho_0}\right)^{\frac{\Gamma^B}{\Gamma}}. \quad (20)$$

The meaning of integration constants is given by Eqs. (18) and (19): at a fixed moment t_0 we have $a(t_0) = a_0$, $\rho(t_0) = \rho_0$, $\rho^B(t_0) = \rho_0^B$, $\Psi(t_0) = \Psi_0$.

Combining Eqs. (15) and (16) and using the radion equation (17) we get the dynamical equation for H ,

$$\dot{H} + 2H^2 = \frac{2}{3}\kappa^2\sigma + \frac{\kappa^2}{6}(\rho - 3p) - \frac{k}{a^2}, \quad (21)$$

which does not contain any additional terms compared with the usual FLRW cosmology. This happens due to the specific form of the coupling function (8) and the potential (11) which cancel all terms containing radion, B-brane matter and B-brane cosmological constant. Yet, the differences from the general relativistic FLRW model are concealed in the bare gravitational constant κ^2 which does not coincide with the Newtonian gravitational constant (see Sect. 6), and also in the form of the constraint equation (15).

In the case $\rho \neq 3p$ ($\Gamma \neq \frac{4}{3}$) the first integral of Eq. (21) reads

$$\frac{d(a^2)}{\sqrt{\sigma a^4 + \rho_0 a_0^{3\Gamma} a^{4-3\Gamma} - \frac{3}{\kappa^2} k a^2 + C a_0^4}} = 2\sqrt{\frac{\kappa^2}{3}} dt, \quad (22)$$

where C is a constant of integration. Using the conservation law (18) it can be written as an expression for the Hubble parameter,

$$H^2 = \frac{\kappa^2}{3}\sigma + \frac{\kappa^2}{3}\rho_0 \left(\frac{a}{a_0}\right)^{-3\Gamma} - \frac{k}{a^2} + \frac{\kappa^2 C}{3} \left(\frac{a}{a_0}\right)^{-4}. \quad (23)$$

The last term is forbidden in the case of the standard FLRW cosmology due to the Friedmann constraint but is allowed in the present case. Let us note that Eq. (23) coincides with the Friedmann equation of the fine-tuned one-brane cosmological model [26] in the low energy approximation where the term $\sim \rho^2$ is neglected. The integration constant C is geometrical in nature and can be interpreted as the value of the energy density of the dark radiation on the A-brane at the moment t_0 .

In the case $\rho = 3p$ ($\Gamma = \frac{4}{3}$) an equation corresponding to Eq. (23) reads

$$H^2 = \frac{\kappa^2}{3} \sigma - \frac{k}{a^2} + \frac{\kappa^2 K}{3} \left(\frac{a}{a_0} \right)^{-4}, \quad (24)$$

where K is an integration constant which can be redefined as a sum of the initial value of radiative matter density ρ_0 and the initial value of the dark radiation density C , $K \equiv \rho_0 + C$. For $k = 0$, $\sigma = 0$ the exact analytic solutions for $a(t)$ and $\Psi(t)$ are presented in Subsect. 4.2.

Eqs. (21), (23) imply an expression for acceleration,

$$\frac{\ddot{a}}{a} = \frac{\kappa^2}{6} ((2 - 3\Gamma)\rho + 2\sigma) - \frac{\kappa^2 a_0^4 C}{3a^4}, \quad (25)$$

which differs from the corresponding expression of the FLRW cosmology only due to the last term. To get an additional drive for acceleration besides the usual cosmological constant, we see the integration constant C must be negative, $C = -|C|$.³ However, in an expanding Universe the last term diminishes quickly in time, so it could have been influential in the early Universe, but is negligible at present.

3.2 Two-brane cosmology in the conformal time

In order to clarify some general properties of the model let us introduce the conformal time on the A-brane, $dt = a(t)d\eta$ as usual, and let us redefine the scalar field as $1 - \Psi = \chi^2$. Then from Eqs. (15)–(17) the following equations follow:

$$(a')^2 - ((a\chi)')^2 + k(a^2 - (a\chi)^2) = \frac{\kappa^2}{3} a^4 (\sigma + \sigma^B \chi^4 + \rho + \rho^B \chi^4), \quad (26)$$

$$a'' + ka = \frac{\kappa^2}{6} a^3 (4\sigma + (4 - 3\Gamma)\rho), \quad (27)$$

$$(a\chi)'' + k(a\chi) = -\frac{\kappa^2}{6} (a\chi)^3 (4\sigma^B + (4 - 3\Gamma^B)\rho^B), \quad (28)$$

with a prime here denoting $d/d\eta$. The result is not surprising taking into account that the B-brane metric is related to the A-brane metric by a conformal transformation with the conformal factor χ^2 .

Dynamical equations (27) and (28) can be integrated and their first integrals read

$$(a')^2 = \frac{\kappa^2}{3} a^4 (\sigma + \rho) - ka^2 + \frac{\kappa^2 a_0^4}{3} C, \quad (29)$$

$$((a\chi)')^2 = -\frac{\kappa^2}{3} (a\chi)^4 (\sigma^B + \rho^B) - k(a\chi)^2 + C^B, \quad (30)$$

where C^B is another constant of integration. Eq. (26) constrains it to be $C^B = \frac{\kappa^2 a_0^4}{3} C$. We see that the influence of the B-brane on the A-brane manifests itself only in permitting

³The same phenomenon was noticed before in the studies of a single brane [27].

non-vanishing values of C which must be proportional to the value of the integration constant C^B in the solution for scale factor ($a\chi$) of the B-brane. If $C = 0$ the cosmologies on the both branes decouple and amount to the usual FLRW models. A non-vanishing C can be interpreted as an initial value of the energy density of the dark radiation on the A-brane (see Subsect. 2.2)

4 Analytic solutions for a flat ($k = 0$) Universe

In general, Eqs. (15)–(17) describe a cosmological model with a two-component source term containing the cosmological constant and a perfect fluid matter ($\Gamma \neq 0$) on both branes. Cosmologically interesting matter tensors are radiation ($\Gamma = 4/3$) and dust ($\Gamma = 1$). However, the full analytic solutions of Eqs. (15)–(17) can be found only in some special cases.

4.1 Cosmological constant dominated Universe

In the case of vanishing matter density ($\rho = 0, p = 0$) and positive cosmological constant on the A-brane ($\sigma > 0$) the solution of Eq. (21) for a flat Universe ($k = 0$) reads⁴

$$H = \begin{cases} \pm\sqrt{\frac{\kappa^2\sigma}{3}} \operatorname{th}\left(\pm 2\sqrt{\frac{\kappa^2\sigma}{3}}(t - t_1)\right) \\ \pm\sqrt{\frac{\kappa^2\sigma}{3}} \operatorname{cth}\left(\pm 2\sqrt{\frac{\kappa^2\sigma}{3}}(t - t_1)\right) \end{cases}, \quad \Longrightarrow \quad a^2 = \begin{cases} a_1^2 \operatorname{ch}\left(\pm 2\sqrt{\frac{\kappa^2\sigma}{3}}(t - t_1)\right) \\ a_1^2 \left| \operatorname{sh}\left(\pm 2\sqrt{\frac{\kappa^2\sigma}{3}}(t - t_1)\right) \right| \end{cases} \quad (31)$$

where a_1, t_1 are integration constants. The solutions (31) approach asymptotically in time the de Sitter solution $H^2 = \frac{\kappa^2}{3}\sigma$, $\sigma > 0$. In an expanding Universe ($H > 0$) the solution $H \sim \operatorname{th}(t)$ is accelerating ($\dot{H} > 0$), while $H \sim \operatorname{cth}(t)$ is decelerating ($\dot{H} < 0$). The influence of the dark radiation can be seen from the first integral (23) where integration constants are included differently,

$$H^2 = \frac{\kappa^2}{3} \left(\sigma + \frac{C a_0^4}{a^4} \right). \quad (32)$$

Here for the expanding Universe the last term on RHS is quickly decaying away leaving simply de Sitter expansion independent of dark radiation.⁵

For negative cosmological constant, $\sigma < 0$, the corresponding solution reads

$$H = \mp\sqrt{\frac{\kappa^2|\sigma|}{3}} \tan\left(\pm 2\sqrt{\frac{\kappa^2|\sigma|}{3}}(t - t_1)\right), \quad \Longrightarrow \quad a^2 = a_1^2 \left| \cos\left(2\sqrt{\pm\frac{\kappa^2|\sigma|}{3}}(t - t_1)\right) \right|. \quad (33)$$

It describes a Universe which contracts into a singularity in finite time.

⁴The solution with th was previously written down in the moduli space approximation [24].

⁵In this case ($C = 0$) an analytic solution also for the scalar field was presented in ref. [21].

4.2 Radiation dominated Universe

In the case $k = 0$, $\Gamma = 4/3$, $\sigma = 0$ Eq. (21) acquires the general relativistic FLRW form,

$$\dot{H} + 2H^2 = 0, \quad \implies \quad \frac{1}{H} - \frac{1}{H_2} = 2(t - t_2), \quad (34)$$

where H_2 , t_2 are constants of integration, $H(t_2) = H_2$. The Hubble parameter decreases ($\dot{H} < 0$) and the scale factor is

$$a = a_2 \sqrt{2H_2(t - t_2) + 1}, \quad (35)$$

where a_2 is a constant of integration, $a(t_2) = a_2$. From Eqs. (34) and (35) the Hubble parameter can be given in terms of the scale factor,

$$H^2 = \frac{H_2^2 a_2^4}{a^4}. \quad (36)$$

Since it must coincide with the first integral (24) the initial value C of the dark radiation density at t_0 can be expressed in terms of integration constants,

$$C + \rho_0 = \frac{3 H_2^2 a_2^4}{\kappa^2 a_0^4}. \quad (37)$$

Eq. (17) for a redefined radion field $\chi^2 \equiv 1 - \Psi$ takes a simple form,

$$\ddot{\chi} + 3H\dot{\chi} = 0, \quad (38)$$

and its solution reads

$$\chi - \chi_\infty = -\frac{g_2}{H_2 \sqrt{2H_2(t - t_2) + 1}}, \quad (39)$$

where χ_∞ and g_2 are integration constants. The constraint equation (15) with $k = 0$, $V = 0$ allows us to determine one of them

$$\Psi_\infty \equiv 1 - \chi_\infty^2 = \frac{\kappa^2}{3H_2^2 a_2^4} (\rho_0 + \rho_0^B \chi_0^4) a_0^4, \quad (40)$$

where ρ_0 , ρ_0^B , χ_0^2 , a_0 are initial values at $t = t_0$ in the solution of the conservation laws (18), (19). In a realistic cosmological model, the radiation dominated era has a finite duration $t \in [t_{in}, t_{out}]$. Substituting $t_2 = t_{in}$ and $H_2 = H_{in}$ into Eqs. (35) and (39), the change in the scalar field can be given in terms of e-folds, $N = \ln(a_{out}/a_{in})$, as

$$\chi_{out} - \chi_{in} = \frac{\dot{\chi}_{in}}{H_{in}} (1 - e^{-N}). \quad (41)$$

If the duration of the radiation dominated era is at least several e-folds, the change of the scalar field is approximately determined only by the values at t_{in} . This also means that after a few e-folds the scalar field remains approximately constant.

The constraint between integration constants (40) can also be used for putting Eq. (36) for H^2 into a form suitable for comparison with general relativity,

$$H^2 = \frac{\kappa^2}{3\Psi_\infty} \left(1 + (1 - \Psi_0)^2 \frac{\rho_0^B}{\rho_0} \right) \rho. \quad (42)$$

Denoting the Hubble parameter of general relativity by H_G and taking into account the standard Friedmann equation $H_G^2 = (8\pi G/3)\rho$ (here G denotes Newtonian gravitational constant which in the context of scalar-tensor theory depends on the asymptotic scalar field, see Subsect. 6.1) the speed-up factor ξ for radiation dominated Universe turns out to be constant,

$$\xi^2 \equiv \frac{H^2}{H_G^2} = \frac{\kappa^2}{8\pi G\Psi_\infty} \left(1 + (1 - \Psi_0)^2 \frac{\rho_0^B}{\rho_0} \right). \quad (43)$$

In terms of the initial values of radiative energy densities ρ_0 , C , it takes a simple form

$$\xi^2 = \frac{\kappa^2}{8\pi G} \left(1 + \frac{C}{\rho_0} \right). \quad (44)$$

Combining the last two equations, one may also express

$$C = \frac{\rho_0(1 - \Psi_\infty) + \rho_0^B(1 - \Psi_0)^2}{\Psi_\infty}. \quad (45)$$

This tells that having dark radiation contributing towards acceleration, i.e., $C < 0$, is only consistent with negative energy density for B-brane radiation, $\rho_0^B < -\frac{1-\Psi_\infty}{(1-\Psi_0)^2}\rho_0$. Yet, since the RHS of Eq. (37) is positive, it is clear that the net contribution of radiation and dark radiation to acceleration is always negative.

4.3 Dust dominated Universe

Integrating the first integral (23) with $k = 0$, $\sigma = 0$, $\Gamma = 1$ leads to a cubic equation for the scale factor which has one real and two complex solutions. The real solution reads

$$a = a_3 \left(\frac{1}{2} b^{\frac{1}{3}} + 2 \frac{C^2}{\rho_0^2} b^{-\frac{1}{3}} + \frac{C}{\rho_0} \right), \quad (46)$$

where t_3 , a_3 are integration constants and the dimensionless quantity b can be written as

$$b = \rho_0^{-3} \left(3\kappa^2 \rho_0^4 (t - t_3)^2 - 8C^3 + \sqrt{9\kappa^4 \rho_0^8 (t - t_3)^4 - 48C^3 \kappa^2 \rho_0^4 (t - t_3)^2} \right). \quad (47)$$

The meaning of t_3 is clarified by the relation $a(t_3) = a_3 \frac{C}{\rho_0}$, which also implies $C \geq 0$. Note that in the case of vanishing dark radiation there is a singularity at the moment t_3 . If $C \neq 0$ and we take t_0 to be the present time, then $t_3 < t_0$, if at present $\frac{C}{\rho_0} < 1$, and $t_3 > t_0$, if $\frac{C}{\rho_0} > 1$.

The Hubble parameter as a function of the cosmic time reads

$$H = \sqrt{\frac{\kappa^2 \rho_0}{3}} \frac{2 \left(1 - 4 \left(\frac{C}{\rho_0} \right)^2 b^{-\frac{2}{3}} \right)}{\sqrt{3\kappa^2 \rho_0 (t - t_3)^2 - 16 \frac{C^3}{\rho_0^3} \left(1 + 2 \left(\frac{C}{\rho_0} \right) b^{-\frac{1}{3}} + 4 \left(\frac{C}{\rho_0} \right)^2 b^{-\frac{2}{3}} \right)}}. \quad (48)$$

In the case of vanishing dark radiation $C = 0$ we get the FLRW value for the Hubble parameter $H = \frac{2}{3}(t - t_3)^{-1}$.

4.4 Universe with cosmological constant and radiation

Eq. (21) with $k = 0$, $\sigma \neq 0$ does not depend on radiation matter with $\Gamma = \frac{4}{3}$, so its solutions coincide with those for cosmological constant dominated Universe (31). In particular, Eq. (32) holds and the late time Universe is dominated by the cosmological constant σ alone.

For getting an equation for the radion field $\chi^2 \equiv 1 - \Psi$ let us solve the corresponding constraint equation (15) as an algebraic equation for $\dot{\chi}$

$$\dot{\chi} = -H\chi \pm \sqrt{H^2 - \frac{\kappa^2}{3}(\rho + \sigma + \chi^4(\rho^B + \sigma^B))}. \quad (49)$$

Taking into account Eq. (32) for H^2 and introducing the conformal time $d\eta = a^{-1}dt$ we get

$$\frac{d}{d\eta}(a\chi) = \pm \frac{\kappa}{\sqrt{3}} \sqrt{(C - \rho_0)a_0^4 + (\sigma^B + \rho_0^B)(a\chi)^4}, \quad (50)$$

which in principle can be integrated in terms of elliptic functions.

5 Evolution of the scalar field

In the previous section it was possible to find analytic solutions for the scale factor since the equations of motion (15)–(17) combined to yield an equation for H decoupled from the scalar field Ψ and B-brane matter. In fact, it is also possible to derive an independent equation for Ψ if we retain only one type of source (cosmological constants or matter) similar on both branes ($\Gamma^B = \Gamma$) and take the Universe to be flat ($k = 0$). Then, after introducing a new time variable [11]

$$dp = h_c dt, \quad h_c = H + \frac{\dot{\Psi}}{2\Psi}, \quad \frac{df}{dp} = f', \quad (51)$$

the equations (15)–(17) together with (20) give a decoupled “master equation” for Ψ ,

$$8(1 - \Psi) \frac{\Psi''}{\Psi} - 3(2 - \Gamma) \left(\frac{\Psi'}{\Psi} \right)^3 - 2 \left((4 - 6\Psi) - (4 - 3\Gamma)(1 - \Psi)W(\Psi) \right) \left(\frac{\Psi'}{\Psi} \right)^2 + 12(2 - \Gamma)(1 - \Psi) \frac{\Psi'}{\Psi} - 8(4 - 3\Gamma)(1 - \Psi)^2 W(\Psi) = 0, \quad (52)$$

where for the cosmological constants ($\Gamma = 0$)

$$W(\Psi) = \frac{1 + (1 - \Psi) \frac{\sigma^B}{\sigma}}{1 + (1 - \Psi)^2 \frac{\sigma^B}{\sigma}}, \quad (53)$$

and for matter ($\Gamma > 0$)

$$W(\Psi) = \frac{1 + (1 - \Psi) \frac{\rho_0^B}{\rho_0} \left(\frac{1 - \Psi}{1 - \Psi_0} \right)^{-\frac{3}{2}\Gamma}}{1 + (1 - \Psi)^2 \frac{\rho_0^B}{\rho_0} \left(\frac{1 - \Psi}{1 - \Psi_0} \right)^{-\frac{3}{2}\Gamma}}. \quad (54)$$

To solve this master equation analytically is still a formidable task, but in order to get a qualitative picture of the evolution of Ψ we can study Eq. (52) as dynamical system.

	Cosmological constants	Interval of Ψ	Allowed region
1)	$\sigma \geq 0, \sigma + \sigma^B \geq 0$	$0 \leq x \leq 1$	$ y \leq 2x\sqrt{1-x} $
2)	$\sigma \geq 0, \sigma + \sigma^B \leq 0$	$0 \leq x \leq 1 - \sqrt{-\frac{\sigma}{\sigma^B}}$ $1 - \sqrt{-\frac{\sigma}{\sigma^B}} \leq x \leq 1$	$ y \geq 2x\sqrt{1-x} $ $ y \leq 2x\sqrt{1-x} $
3)	$\sigma \leq 0, \sigma + \sigma^B \geq 0$	$0 \leq x \leq 1 - \sqrt{-\frac{\sigma}{\sigma^B}}$ $1 - \sqrt{-\frac{\sigma}{\sigma^B}} \leq x \leq 1$	$ y \leq 2x\sqrt{1-x} $ $ y \geq 2x\sqrt{1-x} $
4)	$\sigma \leq 0, \sigma + \sigma^B \leq 0$	$0 \leq x \leq 1$	$ y \geq 2x\sqrt{1-x} $

Table 1: Regions on the $(x = \Psi, y = \Psi')$ plane allowed for dynamics with cosmological constants.

5.1 Cosmological constant dominated Universe

By defining the variables $x \equiv \Psi, y \equiv \Psi'$ we can rewrite the equation (52) for $\Gamma = 0$ as a dynamical system:

$$\begin{aligned} x' &= y \\ y' &= \frac{3y^3}{4x^2(1-x)} + \frac{((4-6x) - 4(1-x)W(x))y^2}{4x(1-x)} - 3y + 4x(1-x)W(x). \end{aligned} \quad (55)$$

The physically allowed regions of the phase space (x, y) are constrained by the Friedmann equation (15), which in terms of the new variables turns out to be

$$h_c^2 = \frac{\kappa^2 (\sigma + (1-x)^2 \sigma^B)}{3x \left(1 - \frac{y^2}{4x^2(1-x)}\right)}. \quad (56)$$

If we let σ and σ^B to take positive and negative values, there are four possibilities, summarized in Table 1. Note, Eq. (56) also assures that the time reparametrization (51) is acceptable — within the borders of the allowed phase space t -time and p -time always run in the same direction.

In order to understand how to read the phase portraits correctly, it is instructive to see how the velocities $\dot{\Psi}$ get mapped to Ψ' by

$$\dot{\Psi} = \frac{d\Psi}{dp} \frac{dp}{dt} = y h_c. \quad (57)$$

It turns out that the boundary

$$B_{\pm} : y = \pm 2x\sqrt{1-x} \quad (58)$$

corresponds to $\dot{\Psi} = \pm\infty$, while $y = 0$ corresponds to $\dot{\Psi} = 0$. The outer reaches, $y = \pm\infty$, which are only relevant when $\sigma + (1-x)^2 \sigma^B < 0$, translate into

$$\dot{\Psi}|_{y=\pm\infty} = \pm\kappa \sqrt{-\frac{4}{3}x(1-x)(\sigma + (1-x)^2 \sigma^B)}, \quad (59)$$

thus we get a minimal bound on the speed of the relative brane motion. At the borders $x = 0$ and $x = 1$ we have $\dot{\Psi} = 0$ and the same holds for the points $(x = 0, y = 0)$ and $(x = 1, y = 0)$ as well. This tells us immediately that the brane collision ($\Psi = 0$) can take place only extremely softly at vanishing relative speed ($\dot{\Psi} \rightarrow 0^-$), and also when the branes approach infinite separation ($\Psi = 1$), they essentially stop moving with respect to each other ($\dot{\Psi} \rightarrow 0^+$). At the crossing points

$$C_{\pm} = \left(x = 1 - \sqrt{-\frac{\sigma}{\sigma^B}}, y = \pm 2 \left(1 - \sqrt{-\frac{\sigma}{\sigma^B}} \right) \sqrt[4]{-\frac{\sigma}{\sigma^B}} \right) \quad (60)$$

the ratio $\frac{dy}{dt}$ becomes undefined, meaning that with our redefinition of time (51) at these values of Ψ all velocities $\dot{\Psi}$ get mapped to a single respective velocity Ψ' .

The system (55) possesses the following fixed points:

- $P_1 = (x = 0, y = 0)$, a saddle point with repulsive and attractive eigenvectors tangential to the upper and lower boundaries B_{\pm} , respectively;
- $P_2 = (x = 1, y = 0)$, a (complex) spiralling attractor, but here the trajectories have to obey also the boundaries of the allowed region;

and in the case $\sigma \geq 0, \sigma + \sigma^B \leq 0$ there is also

- $P_3 = (x = 1 + \frac{\sigma}{\sigma^B}, y = 0)$, a saddle point (having de Sitter expansion for the scale factor [20, 21]).

The limit of general relativity, $\dot{\Psi} = 0, \Psi = 1$, necessarily holds for all trajectories drawn to the right boundary $x = 1$. The phase portraits in the four cases are depicted in Figure 1, let us consider these one by one.

In the case 1) of $\sigma \geq 0, \sigma + \sigma^B \geq 0$ (top left on Figure 1) the allowed phase space is restricted into one bounded region, with $\dot{\Psi} = \pm\infty$ getting mapped to the boundaries B_{\pm} and all the finite values being in the middle. Trajectories can either start near P_1 , where the two branes very close to each other slowly start to move apart, or near P_2 , where the very far away branes slowly begin to move towards each other. The latter class of trajectories will eventually turn around, meaning these branes will never meet but travel back towards infinite separation. Hence all the trajectories are collected by the attractor P_2 , which corresponds to the limit of general relativity. (Of course, by definition the two fixed points provide two stationary trajectories themselves, i.e., two overlapping branes and two infinitely far away branes would always stay so.)

In the case 2) with $\sigma \geq 0, \sigma + \sigma^B \leq 0$ (top right on Figure 1) the allowed phase space consists of three areas, connected via two crossing points C_{\pm} . Notice that in the left areas $\dot{\Psi} = \pm\infty$ gets mapped to the boundaries B_{\pm} , while $y = \pm\infty$ corresponds to a finite velocity (59). Again, the trajectories can either start close to P_1 or close to P_2 . The former trajectories explore the upper left allowed phase space region, pass through the upper crossing point C_+ into the right allowed region and then proceed either to the fixed point P_2 , or pass through the lower crossing point C_- into the lower left allowed region to

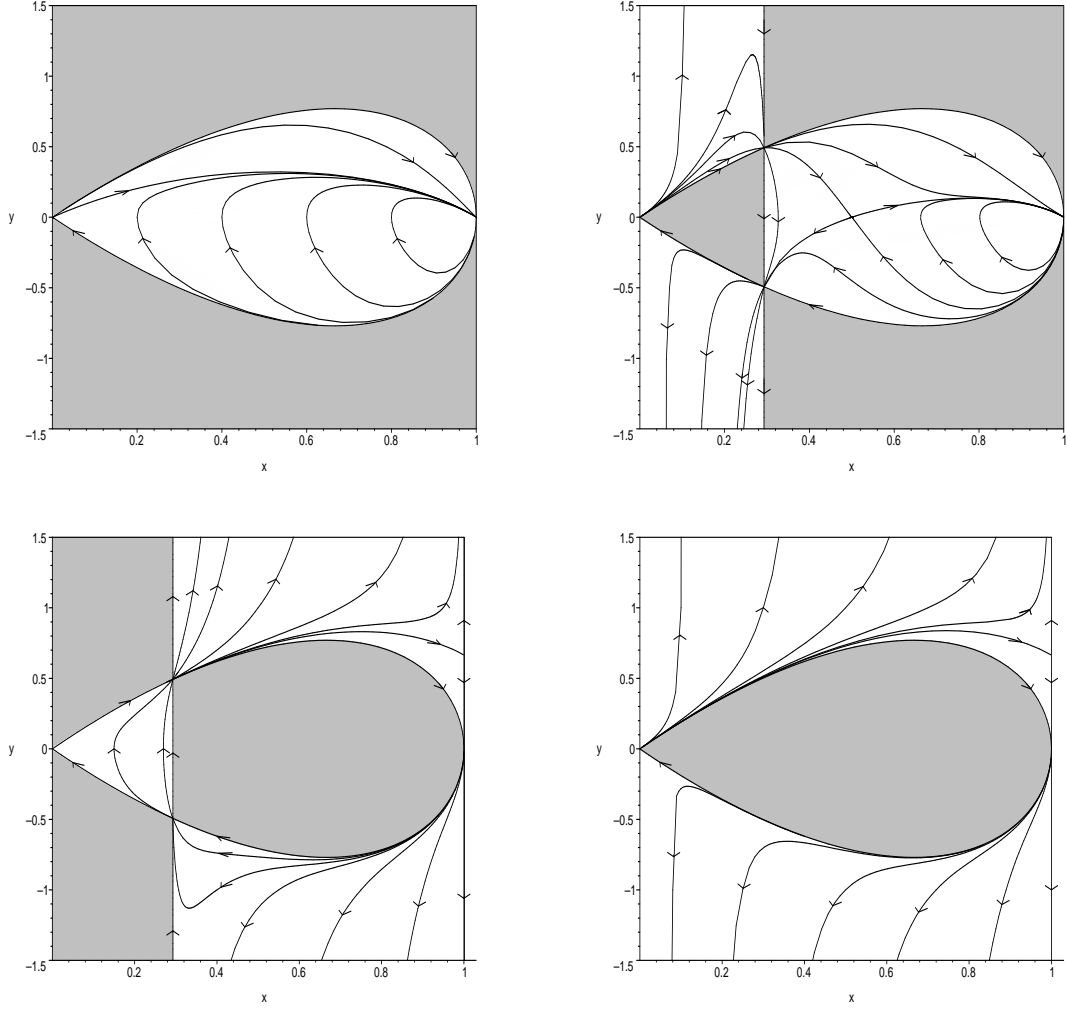


Figure 1: Phase portraits ($x = \Psi(p)$, $y = \Psi'(p)$) for cosmological constants on both branes: 1) $\sigma = 1, \sigma^B = -0.5$ (top, left), 2) $\sigma = 0.5, \sigma^B = -1$ (top, right), 3) $\sigma = -0.5, \sigma^B = 1$ (bottom, left), 4) $\sigma = -1, \sigma^B = 0.5$ (bottom, right).

run into $(x = 0, y = -\infty)$, or in the marginal case terminate at the saddle point P_3 . These correspond to branes either starting very close to each other and moving apart towards infinity, or turning back and colliding, or, marginally, stopping at a finite distance. The other class of trajectories beginning near P_2 have the same possibilities, i.e., either they go back to P_2 , or pass through the crossing point C_- into the lower left region to run into $(x = 0, y = -\infty)$, and there is also a marginal one that terminates at the saddle point P_3 . These correspond to branes starting to move closer to each other from a large distance, and then either separate again, or eventually collide, or in the marginal case come to a standstill at certain finite distance.

In the case 3) with $\sigma \leq 0$, $\sigma + \sigma^B \geq 0$ (bottom left on Figure 1) the allowed regions are an inverse of the previous case. Now the common trajectories may only start near P_2 , explore the lower right region, necessarily pass through C_- , visit the left allowed region,

pass through C_+ , and then either run to P_2 , or to $(x = 1, y = \infty)$, or, marginally, to $(x = 1, y = 2/3)$. These correspond to far apart branes approaching each other to at least a certain distance, and then separating again towards infinity. All these trajectories will gently deliver the limit of general relativity (as they get to $x = 1$). The distinction where they end on the y axis is a coordinate artifact of time p , simply meaning how “fast” their speed measured in time t , i.e., $\dot{\Psi}$ tends to zero.

In the case 4) with $\sigma \leq 0$, $\sigma + \sigma^B \leq 0$ (bottom right on Figure 1) the allowed part of the phase space consists of two separate regions. The trajectories can either begin near P_2 and go to $(x = 0, y = -\infty)$, or start near P_1 and end up at P_2 , $(x = 1, y = 2/3)$, or $(x = 1, y = \infty)$. The former trajectories describe branes coming closer from far apart to a collision, while the latter trajectories describe branes starting very close to each other and moving apart towards infinity, leading to the limit of general relativity.

Some qualitative features of the radion dynamics in the cosmological constants case were inferred previously by Kanno, Soda, and Sasaki [20] by considering the Einstein frame radion potential, and by Webster and Davis [24] in the Jordan frame moduli space approximation. Both papers also point out that the A-brane Hubble parameter does not diverge at the event of brane collision, thus leading to the picture that branes could pass through each other with possible interesting cosmological consequences. Here we observe that the relative brane velocity in the cosmic time slows down and vanishes at the collision. However, this result must be taken with considerable caution, since one expects the effective action to receive corrections near the collision thus changing the behavior of the system [28].

5.2 Radiation dominated Universe

For radiation on both branes ($\Gamma = \Gamma^B = 4/3$) the dynamical system of Eq. (52) reduces to

$$\begin{aligned} x' &= y \\ y' &= \frac{y^3}{4x^2(1-x)} + \frac{(4-6x)y^2}{4x(1-x)} - y. \end{aligned} \quad (61)$$

The Friedmann constraint is similar to the cosmological constants case,

$$h_c^2 = \frac{\kappa^2(\rho + (1-x)^2\rho^B)}{3x\left(1 - \frac{y^2}{4x^2(1-x)}\right)} = \frac{\kappa^2(\rho_0 + (1-\Psi_0)^2\rho_0^B)}{3x\left(1 - \frac{y^2}{4x^2(1-x)}\right)} \left(\frac{a}{a_0}\right)^{-4}, \quad (62)$$

where in the last step we used Eqs. (18), (20) to express ρ and ρ^B . The allowed regions are listed in Table 2, including the exotic possibility of $\rho^B < 0$. The discussion of how $\dot{\Psi}$ is mapped to Ψ' follows along the same lines as before yielding analogous results, only the outer reaches, $y = \pm\infty$, relevant when $\rho_0 + (1-\Psi_0)^2\rho_0^B < 0$, translate into

$$\dot{\Psi}|_{y=\pm\infty} = \pm\kappa\sqrt{-\frac{4}{3}x(1-x)(\rho_0 + (1-\Psi_0)^2\rho_0^B)} \left(\frac{a}{a_0}\right)^{-2}. \quad (63)$$

	Radiation	Interval of Ψ	Allowed region
1)	$\rho^B \geq 0$	$0 \leq x \leq 1$	$ y \leq 2x\sqrt{1-x} $
1a)	$\rho^B < 0, \rho_0 + (1 - \Psi_0)^2 \rho_0^B \geq 0$	$0 \leq x \leq 1$	$ y \leq 2x\sqrt{1-x} $
2)	$\rho^B < 0, \rho_0 + (1 - \Psi_0)^2 \rho_0^B \leq 0$	$0 \leq x \leq 1$	$ y \geq 2x\sqrt{1-x} $

	Dust	Interval of Ψ	Allowed region
1)	$\rho^B \geq 0$	$0 \leq x \leq 1$	$ y \leq 2x\sqrt{1-x} $
1a)	$\rho^B < 0, \rho_0 + (1 - \Psi_0)^{3/2} \rho_0^B \geq 0$	$0 \leq x \leq 1$	$ y \leq 2x\sqrt{1-x} $
2)	$\rho^B < 0, \rho_0 + (1 - \Psi_0)^{3/2} \rho_0^B \leq 0$	$0 \leq x \leq 1 - \frac{\rho_0^2}{\rho_0^{B^2}(1-\Psi_0)^3}$ $1 - \frac{\rho_0^2}{\rho_0^{B^2}(1-\Psi_0)^3} \leq x \leq 1$	$ y \geq 2x\sqrt{1-x} $ $ y \leq 2x\sqrt{1-x} $

Table 2: Regions on the $(x = \Psi, y = \Psi')$ plane allowed for dynamics with radiation and dust (assuming $\rho > 0$).

The limit of general relativity is still approached on the line $x = 1$. However, the main new feature is that the system (61) does not have any fixed points, since the force term has cancelled.

In the case 1) with ρ and ρ^B both positive, and also in the more exotic case 1a) with $\rho^B < 0$, but $\rho_0 \geq (1 - \Psi_0)^2 \rho_0^B$ the allowed phase space covers a single region (Figure 2 top left). The trajectories can either start near $(x = 0, y = 0)$ or $(x = 1, y = 0)$, but all of them end somewhere on the $y = 0$ line. This corresponds to close branes separating or far away branes approaching each other, but eventually all of them slowing down and stopping at some finite distance. The whole dynamics is ruled by friction, which is also in accord with our observation in Subsection 4.2 that after a few e-folds of expansion the scalar field remains approximately constant.

In the other exotic case 2) with $\rho^B < 0$ and $\rho_0 \leq -(1 - \Psi_0)^2 \rho_0^B$ there are two allowed regions (Figure 2 top right). The trajectories beginning near $(x = 0, y = 0)$ run through the upper region into $(x = 1, y = 0)$, meaning close branes separating towards infinity and reaching the limit of general relativity. The trajectories starting near $(x = 1, y = 0)$ run through the lower region into $(x = 0, y = -\infty)$, meaning far away branes coming to collide.

5.3 Dust dominated Universe

Taking both branes to be dominated by dust ($\Gamma = \Gamma^B = 1$) the dynamical system is given by

$$x' = y$$

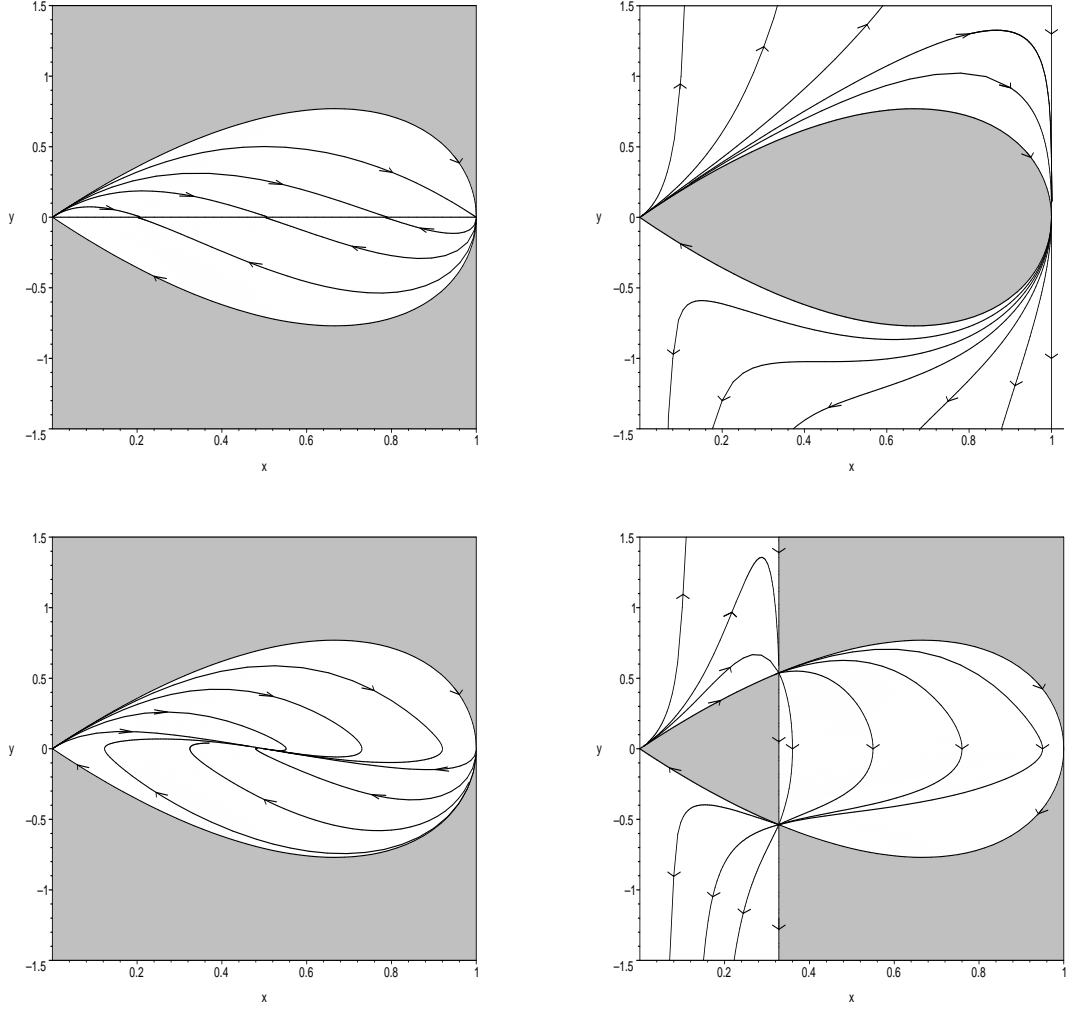


Figure 2: Phase portraits ($x = \Psi(p)$, $y = \Psi'(p)$) for radiation: 1) $\rho = 1, \rho^B = 1, \Psi_0 = 0.1$ (top, left), 2) $\rho_0 = 0.5, \rho_0^B = -1, \Psi_0 = 0.1$ (top, right), and for dust: 1a) $\rho_0 = 0.5, \rho_0^B = -1, \Psi_0 = 0.5$ (bottom, left), 2) $\rho_0 = 0.7, \rho_0^B = -1, \Psi_0 = 0.1$ (bottom, right).

$$y' = \frac{3y^3}{8x^2(1-x)} + \frac{((4-6x) - (1-x)W(x))y^2}{4x(1-x)} - \frac{3y}{2} + x(1-x)W(x). \quad (64)$$

The allowed regions are determined by the Friedmann constraint,

$$h_c^2 = \frac{\kappa^2(\rho + (1-x)^2\rho^B)}{3x\left(1 - \frac{y^2}{4x^2(1-x)}\right)} = \frac{\kappa^2\left(\rho_0 + (1-x)^{1/2}(1-\Psi_0)^{3/2}\rho_0^B\right)}{3x\left(1 - \frac{y^2}{4x^2(1-x)}\right)} \left(\frac{a}{a_0}\right)^{-3}, \quad (65)$$

where again in the last step we used Eqs. (18), (20) to express ρ and ρ^B . The regions available for the dynamics are listed in Table 2. Translating $\dot{\Psi}$ into Ψ' proceeds with analogous results, only the outer reaches, $y = \pm\infty$, relevant when $\rho_0 + (1-\Psi_0)^{3/2}\rho_0^B < 0$, correspond to

$$\dot{\Psi}|_{y=\pm\infty} = \pm\kappa\sqrt{-\frac{4}{3}x(1-x)\left(\rho_0 + (1-x)^{1/2}(1-\Psi_0)^{3/2}\rho_0^B\right)} \left(\frac{a}{a_0}\right)^{-3/2}. \quad (66)$$

The limit of general relativity is $x = 1$ as in the previous cases. The system (64) is endowed with three fixed points:

- $P_1 = (x = 0, y = 0)$, a saddle point with repulsive and attractive eigenvectors tangential to the upper and lower boundaries B_{\pm} , respectively;
- $P_2 = (x = 1, y = 0)$, a (complex) spiralling attractor for $\rho_0^B \geq 0$, but a saddle point for $\rho_0^B < 0$, notice that around here the trajectories have to obey also the boundaries of the allowed region;

and in the case $\rho_0^B < 0$, $\rho_0 + \rho_0^B(1 - \Psi_0)^{3/2} \geq 0$ there exists also

- $P_3 = (x = 1 - \frac{\rho_0^{B2}(1-\Psi_0)^3}{\rho_0^2}, y = 0)$, an attractor.

In the case 1) with $\rho_0 > 0$, $\rho_0^B > 0$ the phase portrait is qualitatively identical to case 1) with cosmological constants (Figure 1 top right). The trajectories can start either at P_1 or P_2 , but they are all attracted to P_2 , approaching the limit of general relativity. The case 1a) with $\rho^B < 0$, $\rho_0 + (1 - \Psi_0)^{3/2} \rho_0^B \geq 0$ offers novel features, since P_2 is now a saddle point, and the dynamics is ruled by the attractor P_3 instead (Figure 2 bottom left). The branes do still start close by (P_1) or very far apart (P_2) but they all eventually move to a finite separation (P_3), determined which does not bring about the limit of general relativity. In the case 2) with $\rho^B < 0$, $\rho_0 + (1 - \Psi_0)^{3/2} \rho_0^B \leq 0$ there is no attractive fixed point (Figure 2 bottom right). Close branes initially separate (P_1), but then meet again at a collision.

Let us point out that taking the B-brane matter to be zero, i.e., considering a scalar-tensor theory with a single usual matter source, corresponds to the case 1) of radiation domination and case 1) of matter domination, yielding qualitatively identical phase portraits in the respective cases. These can be compared with the investigations in general scalar-tensor cosmology [10, 11, 12] carried out in the Einstein frame and using an interpretation of the scalar field in the “master equation” as a coordinate of a fictitious particle with velocity dependent mass. Our results agree – in the radiation domination regime the scalar field slows down and stops due to friction, while in the matter dominated regime it experiences attraction towards general relativity. However, the phase space method delivers an easy to understand global picture without making any approximating assumptions and invoking the unphysical Einstein frame.

6 Observational constraints

6.1 The Eddington parameters and Solar system experiments

The present state of the cosmological scalar field can be detected in the Solar system experiments [13]. Assuming that the B-brane matter has no significant influence on these experiments and taking into account Eq. (8) for $\omega(\Psi)$, the observed values of the

gravitational constant G and the Eddington parameters γ, β read

$$8\pi G \equiv \frac{\kappa^2 (4 + 2\omega_0)}{\Psi_0 (3 + 2\omega_0)} = \kappa^2 \frac{4 - \Psi_0}{3\Psi_0}, \quad (67)$$

$$\gamma - 1 \equiv -\frac{1}{\omega_0 + 2} = -\frac{2(1 - \Psi_0)}{4 - \Psi_0}, \quad (68)$$

$$\beta - 1 \equiv \frac{\kappa^2}{8\pi G} \frac{\omega'(\Psi_0)}{(4 + 2\omega_0)(3 + 2\omega_0)^2} = \frac{2(1 - \Psi_0)\Psi_0}{(4 - \Psi_0)^2}. \quad (69)$$

Here Ψ_0 denotes the cosmological value of the scalar field asymptotically far from Sun and $\omega_0 \equiv \omega(\Psi_0)$. In the case $\Psi_0 = 1$ we get the general relativistic values $\beta = 1 = \gamma$ and $8\pi G = \kappa^2$. But in general $\Psi_0 \neq 1$ and observational limits for $1 - \Psi_0$ can be determined.

The Lunar Laser Ranging experiment (LLR) [29] gives the constraint $4\beta - \gamma - 3 = (-0.7 \pm 1.0) \times 10^{-3}$ and the Shapiro time delay measured by tracking of the Cassini spacecraft [30] gives $\gamma - 1 = (2.1 \pm 2.3) \times 10^{-5}$. In our model $1 - \Psi_0 > 0$ and this implies $4\beta - \gamma - 3 > 0$, $\gamma - 1 < 0$. It follows that in this case the observational bounds are in fact $4\beta - \gamma - 3 < 0.3 \times 10^{-3}$ and $1 - \gamma < 2 \times 10^{-6}$ (cf. [18]). They yield observational limits for the asymptotic value of the scalar field and the modification of the gravitational constant correspondingly

$$1 - \Psi_0 < 10^{-4} \quad (\text{LLR}), \quad 1 - \Psi_0 < 3 \times 10^{-6} \quad (\text{Cassini}); \quad (70)$$

$$\kappa^2/8\pi G < 1 - \frac{4}{3} \times 10^{-4} \quad (\text{LLR}), \quad \kappa^2/8\pi G < 1 - 4 \times 10^{-6} \quad (\text{Cassini}). \quad (71)$$

The constraint on the present variation of $\Psi(t)$ is even more stringent. From the general expression [13]

$$\frac{\dot{G}}{G} \equiv -\dot{\Psi}_0 \frac{3 + 2\omega_0}{4 + 2\omega_0} \left(G + \frac{2\omega'(\Psi_0)}{(3 + 2\omega_0)^2} \right) = -\frac{4\dot{\Psi}_0}{\Psi_0(4 - \Psi_0)} \quad (72)$$

and observational data [13] $|\dot{G}/G| \leq 10^{-11} \text{yr}^{-1}$ we get

$$|\dot{\Psi}_0/\Psi_0| \leq 10^{-11} \text{yr}^{-1}. \quad (73)$$

We can conclude that the asymptotic background for Solar system experiments is very near to general relativity $\Psi = 1$, $\dot{\Psi} = 0$.

6.2 Nucleosynthesis constraints

Primordial big-bang nucleosynthesis (BBN) provides a probe of a very early Universe and gives through primordial (relict) light element abundances (cosmologically relevant are D, ^3He , ^4He , ^7Li) additional constraints for the parameters of the cosmological model under discussion. It can be used to test the non-standard cosmology as well as the non-standard particle physics.

In the framework of general relativity and the standard model of particle physics the relict abundances depend on nuclear reaction rates R_i and only one cosmological

parameter, the ratio of baryon number density n_b to photon number density n_γ , $\eta_{10} \equiv 10^{10} \left(\frac{n_b}{n_\gamma} \right)$. Here we will not discuss here the reaction rate uncertainties ΔR_i , for a recent review, see [31]. Modifications of the standard cosmological model and the standard model of particle physics can be given in terms of two additional parameters: 1) the lepton asymmetry parameter (asymmetry between neutrinos and antineutrinos or neutrino degeneracy) ξ_e [32]; 2) the speed-up factor $\xi(t) = H(t)/H_G(t)$ (in the framework of our model we considered it in Subsect. 4.2 for the radiation dominated Universe).

Kneller and Steigman [33] have presented the primordial abundances $\{y_D, Y_P, y_{Li}\}$ of $\{D, {}^4\text{He}, {}^7\text{Li}\}$ as linear functions of parameters $\{\eta_{10}, \xi, \xi_e\}$ where $\xi = \xi(t_{nucleosynth})$. The accuracy of these linear fits is approximately a few percent (lower than the current errors in observationally inferred value) over realistic ranges of parameters [32, 33] $4 \leq \eta_{10} \leq 8$, $0.85 \leq \xi \leq 1.15$, $-0.1 \leq \xi_e \leq 0.1$. The baryon to photon ratio η_{10} is determined at high precision from independent (non-BBN) measurements of CMB made by WMAP. In the standard Λ CDM theoretical model its value is $\eta_{10} = 6.14 \pm 0.25$ and it is approximately the same also in the case of nonstandard cosmological models [33]. We can take into account this (non-BBN) value and observed abundances of three elements, but then we cannot adjust the remaining two parameters $\{\xi, \xi_e\}$ so that all three fits are satisfied. Since the lithium abundance derived from observations has possible problems, Kneller and Steigman [33] derive possible values of the parameters only from D and ${}^4\text{He}$ abundances in two cases:

- if $\xi_e = 0$, then $\eta_{10} = 5.88_{-0.50}^{+0.64}$ and $\xi = 0.969_{-0.009}^{+0.008}$;
- if $\eta_{10} = 6.14$, then $\xi_e \approx 0.037$ and $\xi \approx 1.0203$.

Now let us proceed with our specific scalar-tensor theory with coupling function (8). The nucleosynthesis takes place at the beginning of the radiation dominated era and then the influence of the cosmological constant is negligible, so the relevant speed-up factor is given by Eq. (44). The range of realistic values [33] $0.85 \leq \xi \leq 1.15$ translates for C/ρ_0 as

$$-0.28 < \frac{C}{\rho_0} < 0.32 \quad (74)$$

(small corrections from $\kappa^2/8\pi G$ ignored) and above-given observational constraints [33] on ξ yield

- for $\xi \approx 0.969$ we get $C/\rho_0 \approx -0.063$;
- for $\xi \approx 1.0203$ we get $C/\rho_0 \approx 0.041$.

The initial value of the dark energy density as a fraction of the background radiative matter energy density C/ρ_0 is sometimes parametrized by the number of extra relativistic degrees of freedom, conventionally represented as additional neutrino flavors, $\Delta N_\nu \equiv (N_\nu - 3)$. In this case the speed-up factor reads [33]

$$\xi^2 = \frac{\kappa^2}{8\pi G} \left(1 + \frac{7}{43} \Delta N_\nu \right) \quad \implies \quad \frac{C}{\rho_0} = \frac{7}{43} \Delta N_\nu . \quad (75)$$

Note that in our model the dark radiation is of geometric nature and its parametrization in terms of additional neutrino flavors is absolutely formal.

Using updated predictions for light element abundances, BBN and CMB limit Cyburt et al. [34, 35] infer a combined limit $-0.33 \leq \Delta N_\nu \leq 0.85$, meaning

$$-0.054 \leq \frac{C}{\rho_0} \leq 0.138. \quad (76)$$

This result can be compared with limits given by Ichiki et al. [36] for the ratio of dark and visible radiation in the framework of an one-brane model in an approximation $\rho^2 \approx 0$, since in this case H^2 and ξ^2 coincide with the corresponding expressions in our two-brane model. Ichiki et al. [36] derived from BBN and CMB $-0.41 \leq \frac{C}{\rho_0} \leq 0.105$ (using $4.73 \leq \eta_{10} \leq 5.56$). We see that limits for the positive dark energy are approximately the same, but the negative dark energy density is much more constrained by Eq. (76).

Finally let us note that the observational limits (76) imply constraints on the parameters of the cosmological model in the radiation dominated era, as

$$\frac{C}{\rho_0} = \frac{\rho_0 + \rho_0^B (1 - \Psi_0)^2}{\rho_0 \Psi_\infty} - 1 \quad (77)$$

from Eq. (45). For example, we can determine immediately that the case 2) with $\rho^B < 0$, $\rho_0 + (1 - \Psi_0)^2 \rho_0^B \leq 0$, discussed in Subsec. 5.2, is by far ruled out by the observations.

7 Concluding remarks

In this paper we have investigated a scalar-tensor cosmology arising as an effective 4-dimensional description of the 5-dimensional Randall-Sundrum two-brane cosmological scenario [1] in the Kanno-Soda low energy gradient expansion approximation [7]. The model is characterized by a scalar field Ψ (radion) measuring the proper distance of the branes and endowed with a specific coupling function (8) implied by the construction of the model, a specific potential (11) generated by cosmological constants on the branes, and barotropic fluid matter sources on both branes. In the limit when the (hidden) B-brane is empty, the model reduces to a scalar tensor cosmology with cosmological constant and matter, the limit of general relativity is obtained when $\Psi = 1, \dot{\Psi} = 0$. We have assumed FLRW metric on both branes.

Due to the specific form of the coupling function the Jordan frame equations of motion combine to give a scale factor dynamical equation decoupled from the scalar field and B-brane matter, leading to a Friedmann equation with only an additional dark radiation term reminding the extra dimension. This has enabled us to find exact analytic solutions for the flat ($k = 0$) Universe scale factor with various kinds of matter: cosmological constant, radiation, dust, and cosmological constant plus radiation. We have also found analytic solutions for the scalar field with radiation, and with cosmological constant plus radiation (latter case to be expressed in terms of elliptic functions). Over the years Barrow et al. have developed methods to obtain exact analytic solutions for scalar tensor

cosmologies with general coupling functions [13, 38]. Forgetting the B-brane component, our model belongs to classes 1 and 3 studied in ref. [13]. However, in the general case the solutions are not explicitly available in the cosmic time and one resorts to approximation techniques for early and late time behavior. Therefore, despite being a specific one, our model has an advantage of being directly solvable, thus providing an interesting example of a scalar-tensor cosmology throughout the entire radiation, dust and cosmological constant dominated eras.

Although our model is governed by the Friedmann equation (with an extra dark radiation term) and hence in broad accordance with standard cosmology, we need to study the behavior of the scalar field, in order to be assured that the theory satisfies all observational constraints and converges towards general relativity. A clever reparametrization of time [11] allows to extract an independent evolution equation for the scalar field also when besides matter on the A-brane, there is similar matter ($\Gamma^B = \Gamma$) on the B-brane. We examine the solutions of this “master equation” by applying the methods of dynamical systems. It seems determining the fixed points and drawing the phase portraits is a more straightforward approach than the usual procedure of changing into the unphysical Einstein frame and relying on an analogue with a fictitious particle with velocity dependent mass. Still, in the absence of B-brane matter, the results are in accord with previous general studies [10, 12, 11]: in a flat Universe with positive cosmological constant or dust the system relaxes to the limit of general relativity, while in the radiation case friction makes the scalar field to stop at an arbitrary position.

Inclusion of the B-brane matter (possibly having negative energy density) complicates the story, as was also previously noted from the numerical studies in the moduli space approximation approach [8]. In summary, we find that general relativity, which in the branes’ picture corresponds to infinitely far away branes, is the sole destiny for cosmological constants $\sigma + \sigma^B \geq 0$, or dust $\rho_0 \geq 0$, $\rho_0^B \geq 0$. The solutions may approach general relativity or go the other way, i.e., to brane collision, depending on the initial conditions, for cosmological constants $\sigma + \sigma^B \leq 0$, or radiation $\rho_0 + (1 - \Psi_0)^2 \rho_0^B \leq 0$. Brane collision is the only future for dust with $\rho_0 + (1 - \Psi_0)^{3/2} \rho_0^B \leq 0$. Radiation with $\rho_0 + (1 - \Psi_0)^2 \rho_0^B \geq 0$ has the radion stabilizing at arbitrary position due to friction. There are also fixed points in between the two extremes, namely a saddle for cosmological constants $\sigma > 0$, $\sigma + \sigma^B \leq 0$, and an attractor for dust $\rho_0^B < 0$, $\rho_0 + (1 - \Psi_0)^{3/2} \rho_0^B \geq 0$. The latter is especially interesting, since we see a natural stabilization of the radion for which one usually invokes an additional scalar field in the bulk [39].

The solar system tests restrict the present value of the radion to $1 - \Psi < 10^{-4}$, and allow it to be only very slowly varying, $|\dot{\Psi}/\Psi| \leq 10^{-11} \text{yr}^{-1}$. The observations of D and He abundances together with CMB set limits on the fraction of dark radiation to normal radiation, $-0.054 \leq \frac{C}{\rho_0} \leq 0.138$. The results of these experiments can be accommodated in the model if its parameters are correspondingly constrained, which is not too hard, given that for large range of parameters general relativity is an attractor. Due to the specific coupling function (8) the first integral (23) for the two-brane cosmology coincides with

the Friedmann equation for the one-brane cosmology [26] in the approximation where the matter density ρ on the brane is small and quadratic term ρ^2 can be neglected. This means that observational constraints for our model can be analyzed along the same patterns as in the case of the one-brane cosmology [36, 37]. Also note that the specific coupling (8) implies constant speed-up factor (43) in the radiation dominated era and excludes a variable speed-up factor mechanism recently proposed by Larena et al. [40] for solving the Li abundance problem.

References

- [1] L. Randall and R. Sundrum, Phys. Rev. Lett. 83: 3370 (1999), [hep-ph/9905221].
- [2] L. Randall and R. Sundrum, Phys. Rev. Lett. 83: 4690 (1999), [hep-th/9906064].
- [3] A. Lukas, B.A. Ovrut, K.S. Stelle, and D. Waldram, Phys. Rev. D 59: 086001 (1999), [hep-th/9803235].
- [4] J. Khoury, B. Ovrut, P.J. Steinhardt, and N. Turok, Phys. Rev. D 64: 123522 (2001), [hep-th/0103239].
- [5] S. Kanno, J.Soda, and D. Wands, JCAP 0508: 002 (2005), [hep-th/0506167].
- [6] S. Kanno and J. Soda, Phys. Rev. D 66: 043526 (2002), [hep-th/0205188].
- [7] S. Kanno and J. Soda, Phys. Rev. D 66: 083506 (2002), [hep-th/0207029].
- [8] Ph. Brax, C. van de Bruck, A.-C. Davis, and C.S. Rhodes, Phys. Rev. D 67: 023512 (2003), [hep-th/0209158].
- [9] S. Kanno, Phys. Rev. D 72: 024009 (2005), [hep-th/0504087].
- [10] T. Damour and K. Nordtvedt, Phys. Rev. D 48: 3436 (1993).
- [11] A. Serna, J.M. Alimi, and A. Navarro, Class. Quant. Grav. 19: 857 (2002), [gr-qc/0201049].
- [12] D.I. Santiago, D. Kalligas, and R.W. Wagoner, Phys. Rev. D 58: 124005 (1998), [gr-qc/9805044].
- [13] J.D. Barrow and P. Parsons, Phys. Rev. D 55: 1906 (1997), [gr-qc/9607072].
- [14] D.I. Santiago, D. Kalligas, and R.W. Wagoner, Phys. Rev. D 56: 7627 (1997), [gr-qc/9706017].
- [15] T. Damour and B. Pichon, Phys. Rev. D 59: 123502 (1999), [astro-ph/9807176].
- [16] T. Clifton, J.D. Barrow, and R.J. Scherrer, Phys. Rev. D 71: 123526 (2005), [astro-ph/0504418].

- [17] A. Coc, K.A. Olive, J.-P. Uzan, and E. Vangioni, *Phys. Rev. D* 73: 083525 (2006), [astro-ph/0601299].
- [18] G.A. Palma, *Phys. Rev. D* 73: 044010 (2006), [hep-th/0511170].
- [19] V. Faraoni, “Cosmology in scalar tensor gravity”, Dordrecht, Netherlands: Kluwer Academic Publishers (2004).
- [20] S. Kanno, M. Sasaki, and J. Soda, *Prog. Theor. Phys.* 109: 357 (2003), [hep-th/0210250].
- [21] P. Kuusk and M. Saal, *Gen. Rel. Grav.* 36: 1001 (2004), [gr-qc/0309084].
- [22] C. Csaki, M. Graesser, C.F. Kolda, and J. Terning, *Phys. Lett. B* 462: 34 (1999), [hep-ph/9906513].
 J. M. Cline, C. Grojean, and G. Servant, *Phys. Rev. Lett.* 83: 4245 (1999), [hep-ph/9906523].
 P. Binétruy, C. Deffayet, U. Ellwanger, and D. Langlois, *Phys. Lett. B* 477: 285 (2000), [hep-th/9910219].
 C. Csaki, M. Graesser, L. Randall, and J. Terning, *Phys. Rev. D* 62: 045015 (2000), [hep-ph/9911406].
 P. Binétruy, C. Deffayet, and D. Langlois, *Nucl. Phys. B* 615: 219, (2001), [hep-th/0101234].
 K. Koyama, *Phys. Rev. D* 66: 084003 (2002), [gr-qc/0204047].
 S. Kobayashi and K. Koyama, *JHEP* 0212: 056 (2002), [hep-th/0210029].
 I. Brevik, K. Borkje, and J.P. Morten, *Gen. Rel. Grav.* 36: 2021 (2004), [gr-qc/0310103].
 J. Martin, G.N. Felder, A.V. Frolov, M. Peloso, and L. Kofman, *Phys. Rev. D* 69: 084017 (2004), [hep-th/0309001].
 J. Martin, G.N. Felder, A.V. Frolov, L. Kofman, and M. Peloso, *Comput. Phys. Commun.* 171: 69 (2005), [hep-ph/0404141].
 A. Wang, R.G. Cai, and N.O.Santos, [astro-ph/0607371].
- [23] G.A. Palma and A.C. Davis, *Phys. Rev. D* 70: 064021 (2004), [hep-th/0406091].
- [24] S.L. Webster and A.C. Davis, [hep-th/0410042].
- [25] J. Garriga and T. Tanaka, *Phys. Rev. Lett.* 84: 2778 (2000), [hep-th/9911055].
- [26] P. Binétruy, C. Deffayet, U. Ellwanger, and D. Langlois, *Phys. Lett. B* 477: 285 (2000), [hep-th/9910219].

- [27] E. Kiritsis, G. Kofinas, N. Tetradis, T.N. Tomaras, and V. Zarikas, JHEP 0302: 035 (2003), [hep-th/0207060].
 N. Tetradis, Phys. Lett. B 569: 1 (2003), [hep-th/0211200].
 K. I. Umezumi, K. Ichiki, T. Kajino, G.J. Mathews, R. Nakamura, and M. Yahiro, Phys. Rev. D 73: 063527 (2006), [astro-ph/0507227].
 P.S. Apostolopoulos and N. Tetradis, Phys. Lett. B 633: 409 (2006), [hep-th/0509182].
- [28] T. Shiromizu, K. Koyama, and K. Takahashi, Phys. Rev. D 67: 104011, (2003), [hep-th/0212331].
 C. de Rham and S. Webster, Phys. Rev. D 71: 124025 (2005), [hep-th/0504128].
 C. de Rham and S. Webster, Phys. Rev. D 72: 064013 (2005), [hep-th/0506152].
 C. de Rham, S. Fujii, T. Shiromizu, and H. Yoshino, Phys. Rev. D 72: 123522 (2005), [hep-th/0509194].
- [29] J. G. Williams, X. X. Newhall, and J. O. Dickey, Phys. Rev. D 53: 6730 (1996).
- [30] B. Bertotti, L. Iess, and P. Tortora, Nature 425: 374 (2003).
- [31] R. Cyburt, Phys. Rev. D 70: 023505 (2005), [astro-ph/0401091].
- [32] G. Steigman, Int. J. Mod. Phys. E 15: 1 (2006), [astro-ph/0511534].
- [33] J.P. Kneller and G. Steigman, New J. Phys. 6: 117 (2004), [astro-ph/0406320].
- [34] R.H. Cyburt, B.D. Fields, and K.A. Olive, Phys. Lett. B 567: 227 (2003), [astro-ph/0302431].
- [35] R.H. Cyburt, B.D. Fields, K.A. Olive, and E. Skillman, Astropart. Phys. 23: 313 (2005), [astro-ph/0408033].
- [36] K. Ichiki, M. Yahiro, T. Kajino, M. Orito, and G.J. Mathews, Phys. Rev. D 66: 043521 (2002), [astro-ph/0203272].
- [37] J.D. Bratt, A.C. Gault, R.J. Scherrer, and T.P. Walker, Phys. Lett. B 546: 19 (2002), [astro-ph/0208133].
- [38] J.D. Barrow, K. Maeda, Nucl. Phys. B 341: 294 (1990).
 J.D. Barrow, Phys. Rev. D 47: 5329 (1993).
 J.D. Barrow, J. Mimoso, Phys. Rev. D 50: 3746 (1994).
- [39] W.D. Goldberger, M.B. Wise, Phys. Rev. Lett. 83: 4922 (1999), [hep-ph/9907447].
- [40] J. Larena, J.-M. Alimi, and A. Serna, (submit. to Phys. Rev. D), [astro-ph/0511693].